Supercritical water gasification of sewage sludge in continuous reactor
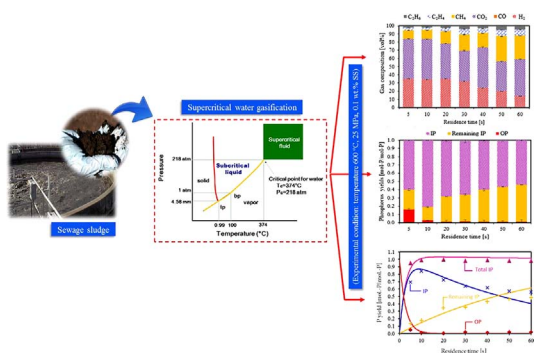
Apip Amrullah[a,b], Yukihiko Matsumura[a,*]

[a] Department of Mechanical Science and Engineering, Hiroshima University, 1-4-1 Kagamiyama, Higashi-Hiroshima 739-8527, Japan
[b] Original affiliation: Department of Mechanical Engineering, Universitas Lambung Mangkurat, Banjarmasin, South Kalimantan, Indonesia

GRAPHICAL ABSTRACT

ARTICLE INFO

ABSTRACT

In this study, a process for the continuous recovery of phosphorus and generation of gas from sewage sludge is investigated for the first time using supercritical water gasification (SCWG). A continuous reactor was employed and experiments were conducted by varying the temperature (500–600 °C) and residence time (5–60 s) while fixing the pressure at 25 MPa. The behavior of phosphorus during the SCWG process was studied. The effect of the temperature and time on the composition of the product gas was also investigated. A model of the reaction kinetics for the SCWG of sewage sludge was developed. The organic phosphorus (OP) was rapidly converted into inorganic phosphorus (IP) within a short residence time of 10 s. The gaseous products were mainly composed of H_2, CO_2, and CH_4. The reaction followed first order kinetics, and the model was found to fit the experimental data well.

1. Introduction

The effort to mitigate climate change has driven increasing research on biomass utilization as an alternative source of renewable energy. Sewage sludge is considered as a promising biomass source for conversion to energy as it contains inorganic matter such as nitrogen and phosphorus and organic compounds such as proteins (± 40%), lipids (10–25%), carbohydrates (14%), and lignins (30–50%) (Goto et al., 1999). Various techniques for converting sewage sludge into useful secondary energy via pyrolysis (Deng et al., 2017; Liu et al., 2017), combustion, and supercritical water gasification (SCWG) have been developed (Han et al., 2017; He et al., 2014; Petzet et al., 2012; Qian et al., 2017; Yanagida et al., 2008). However, sewage sludge has a moisture content of up to 85 wt%, which leads to high drying costs when pyrolysis or combustion is employed. In contrast, SCWG is suitable for converting biomass containing high-moisture compounds such as sewage sludge, as the gasification reaction takes place in water, and pre-drying the biomass is not required (Farobie et al., 2017). Under

1. Water
2. Pump
3. Feeding system
4. Furnace
5. Reactor
6. Temperature controller
7. Heat exchanger
8. Cooling system
9. Filter
10. Back pressure regulator
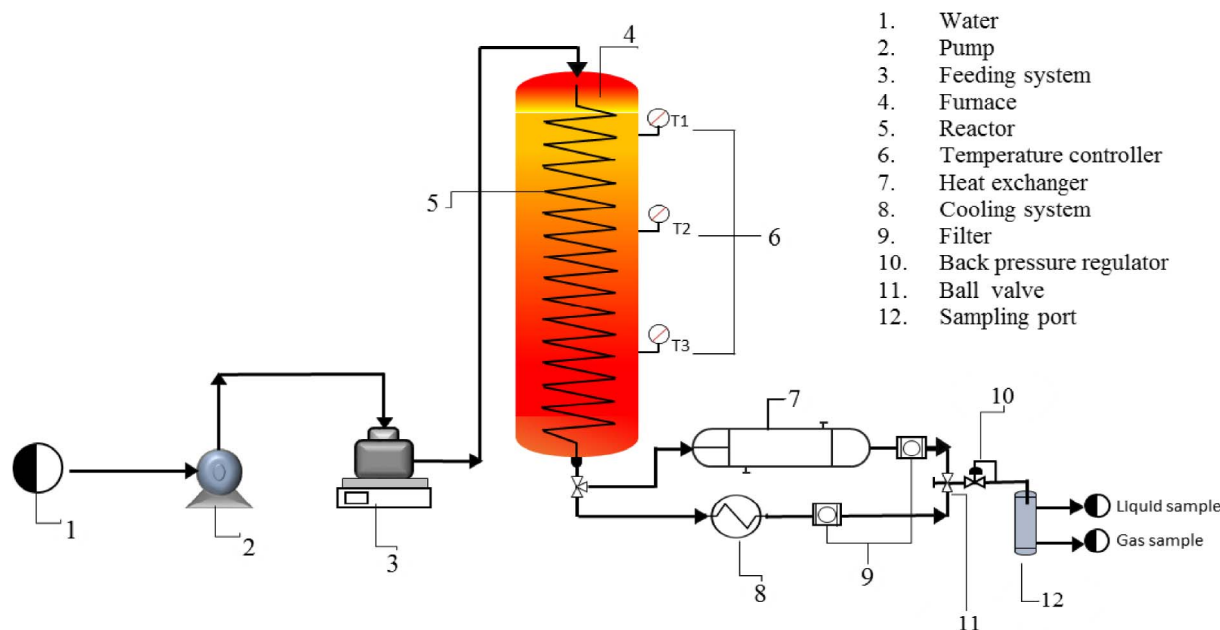11. Ball valve
12. Sampling port

Fig. 1. Experimental apparatus.

these conditions, water has great potential as a solvent for organic components and gases because all of the fluids remain in a single phase (Kruse and Dinjus, 2007; Matsumura et al., 2005; Paksung and Matsumura, 2015; Samanmulya et al., 2017; Yanagida et al., 2008).

Extensive studies on the conversion of sewage sludge into secondary energy using SCWG have been conducted, with focus on gas production. In pioneering studies, Xu et al. (1996) evaluated the SCWG of sewage sludge. Recently, Zhang et al. (2010) reported that supercritical water (SCW) is able to transform sewage sludge into fuel gases such as H_2, CO, and CH_4 with reduced tar and coke formation compared to the traditional thermal processes. Xu et al. (2013) investigated the effect of alkali salts on the direct gasification of sewage sludge in SCW. The hydrogen yield increased in the presence of alkali salts (NaOH, KOH, K_2CO_3, and Na_2CO_3), except for $Ca(OH)_2$. Gong et al. (2016) studied the influence of the reactant composition, i.e., carbon-hydrogen-oxygen, on the key products of the direct gasification of dewatered sewage sludge in a high-pressure autoclave. The total gas production increased with an increase in the C/H_2O ratio of the reactant.

Considering that the recovery of phosphorus from sewage sludge is also important due to the depletion of mineral phosphorus resources, studies on phosphorus recovery from sewage sludge are urgently required. Arakane et al. (2005) recovered phosphorus from excess sludge by applying a process employing subcritical water with magnesium ammonium phosphate (MPA). Yuan et al. (2012) studied the recovery of phosphorus from wastewater through microbial processes, known as enhanced biological phosphorus removal (EBPR). Blöcher et al. (2012) investigated phosphorus recovery from sewage sludge by employing a hybrid process involving low-pressure wet oxidation and nanofiltration. A phosphorus recovery of 54% was obtained in an example of wastewater treatment.

To make sewage sludge treatment energetically efficient, a process for the simultaneous recovery of phosphorus and gas production is needed. A few studies have attempted to recover phosphorus and to generate syngas simultaneously by using SCWG. Thus far, the gasification of dewatered sewage sludge in SCW for energy recovery combined with phosphorus recovery has only been attempted by Acelas et al. (2014). However, a batch reactor was employed in their study. To the best of our knowledge, there are no comprehensive studies on gas generation combined with phosphorus recovery as well as detailed analysis of the reaction kinetics for the SCWG of sewage sludge using a

continuous reactor. By employing a continuous reactor, the pressure can be constantly controlled and elucidation of the reaction kinetics is much more precise than in the case of a batch reactor. Therefore, this study aims to investigate the behavior of phosphorus during the SCWG of sewage sludge to determine the effect of temperature and time on the product gas composition and to evaluate the kinetics of sewage sludge conversion under SCWG conditions.

2. Materials and methods

2.1. Experimental

The SCWG of sewage sludge was carried out in a continuous mode reactor. A schematic of the experimental apparatus is shown in Fig. 1. The reactor was made of SS316 steel tubing (i.d. 2.17 mm, o.d., 3.18 mm, and length 12 m). The reactor was placed inside an electric furnace. To start up the experimental setup, water was fed into the reactor. Subsequently, the pressure was adjusted to 25 MPa using a back-pressure regulator. After achieving a constant pressure of 25 MPa, the reactor temperature was set to the desired temperature. The feedstock was then fed using a feeding system at an agitation speed of 400 rpm, with a range of feedstock flowrate of 1.3–15 mL/min. The residence time was changed in the range of 5–60 s. The density of water is 89.74, 78.52 and 70.72 kg/m^3 at the temperature of 500, 550 and 600 °C respectively. After the reactor reached the desired experimental conditions, the feedstock was fed into the system. To ensure steady-state conditions, the reactor was operated for 1 h prior to sample collection. All reaction products were cooled in the heat exchanger, and when a constant gas generation rate was achieved, gas samples were collected in vials and their compositions were determined. Liquid samples were also collected to determine the total organic carbon (TOC) content. All measurements were conducted in triplicate, and the average was taken.

Partial precipitation of phosphorus in the reactor was observed, and the precipitate was recovered after the experimental run. To recover this precipitate, water was fed into the reactor while cooling the reactor, and the effluent generated during this cooling stage was also collected and analyzed.

The residence time was determined using Eq. (1), assuming there was no volume change caused by mixing. The reactor volume here is
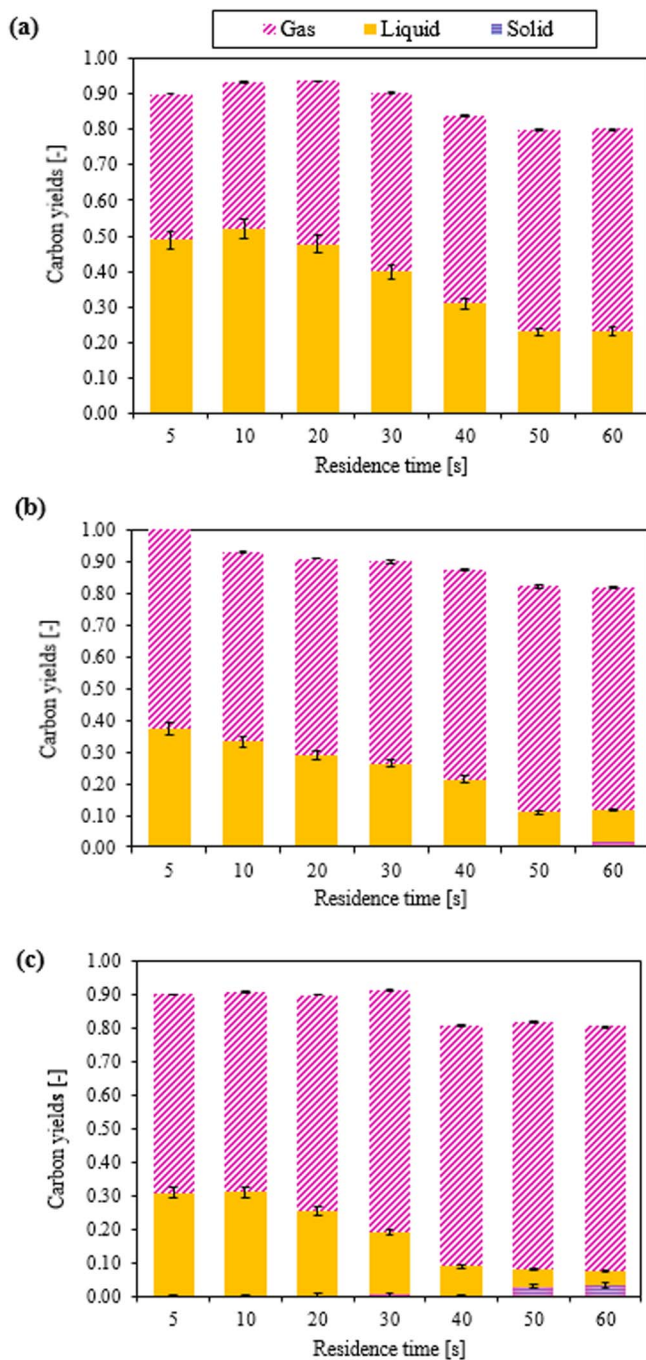
Fig. 2. Carbon yield of sewage sludge gasification at the reaction temperatures of (a) 500 °C, (b) 550 °C, and (c) 600 °C.

Fig. 3. Phosphorus yield of sewage sludge gasification at the reaction temperatures of (a) 500 °C, (b) 550 °C, and (c) 600 °C.

the volume of a portion of the reactor with a length of 12.0 m,

$$\tau = \frac{V}{(m_{fw}/\rho_w)} \qquad (1)$$

where, τ is the residence time [s], V is the reactor volume [m^3], m_{fw} is the mass flow rate of the water [kg/s], and ρ_w is the density of water [kg/m^3].

2.2. Analytical method

The liquid samples were analyzed using a total organic carbon (TOC) analyzer to quantify the amount of carbon in the liquid product (non-purgeable organic carbon or NPOC) and in the dissolved gas
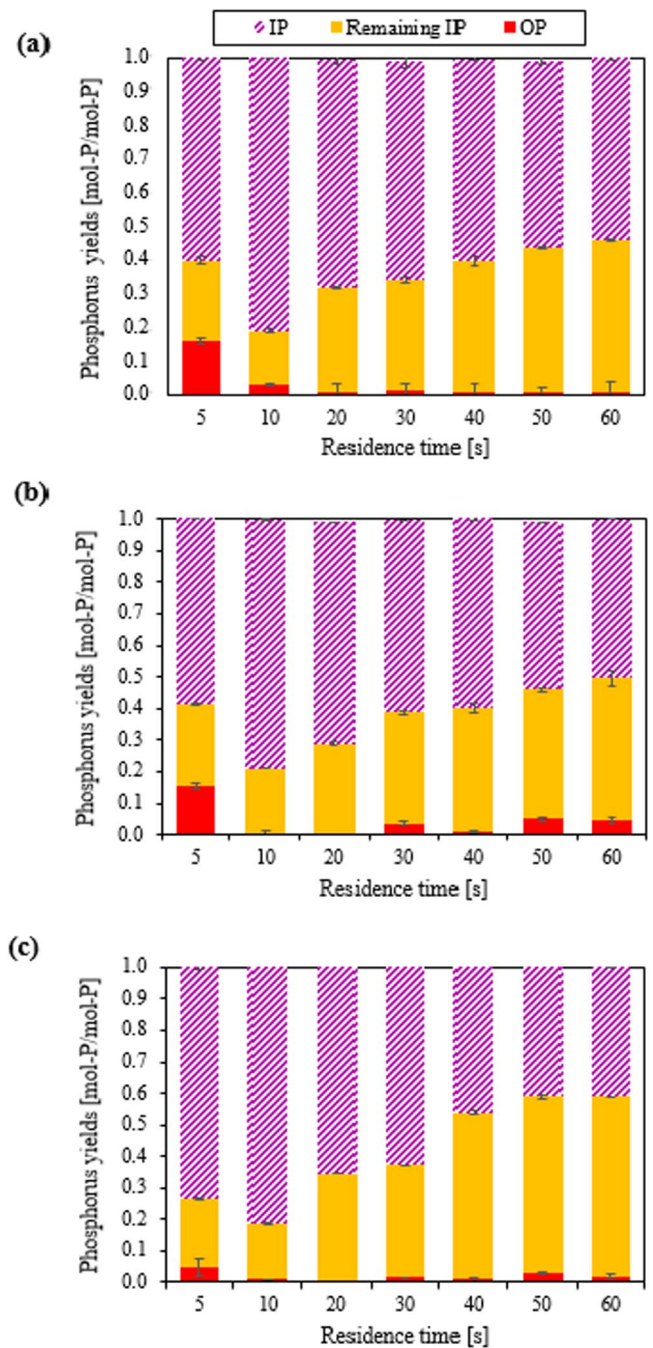
product (inorganic carbon or IC). The phosphorus yield in the liquid phase was determined by using ion chromatography (IC) to quantify the inorganic phosphorus (IP) and the molybdenum blue method to quantify the total phosphorus (TP). The molybdenum blue method was adopted from a previous study (Zhu et al., 2011). The IP and TP yields were determined using Eqs. (2) and (3), respectively.

$$\text{IP yield}\,[-] = \frac{(\text{IP in liquid sample}\,[\text{mol}-\text{P}])}{(\text{TP in feedstock}\,[\text{mol}-\text{P}])} \qquad (2)$$

$$\text{TP yield}\,[-] = \frac{(\text{TP in liquid sample}\,[\text{mol}-\text{P}])}{(\text{TP in feedstock}\,[\text{mol}-\text{P}])} \qquad (3)$$

The organic phosphorus (OP) yield was obtained by subtracting the IP yield from the TP yield. The effluent from the cooling stage was also
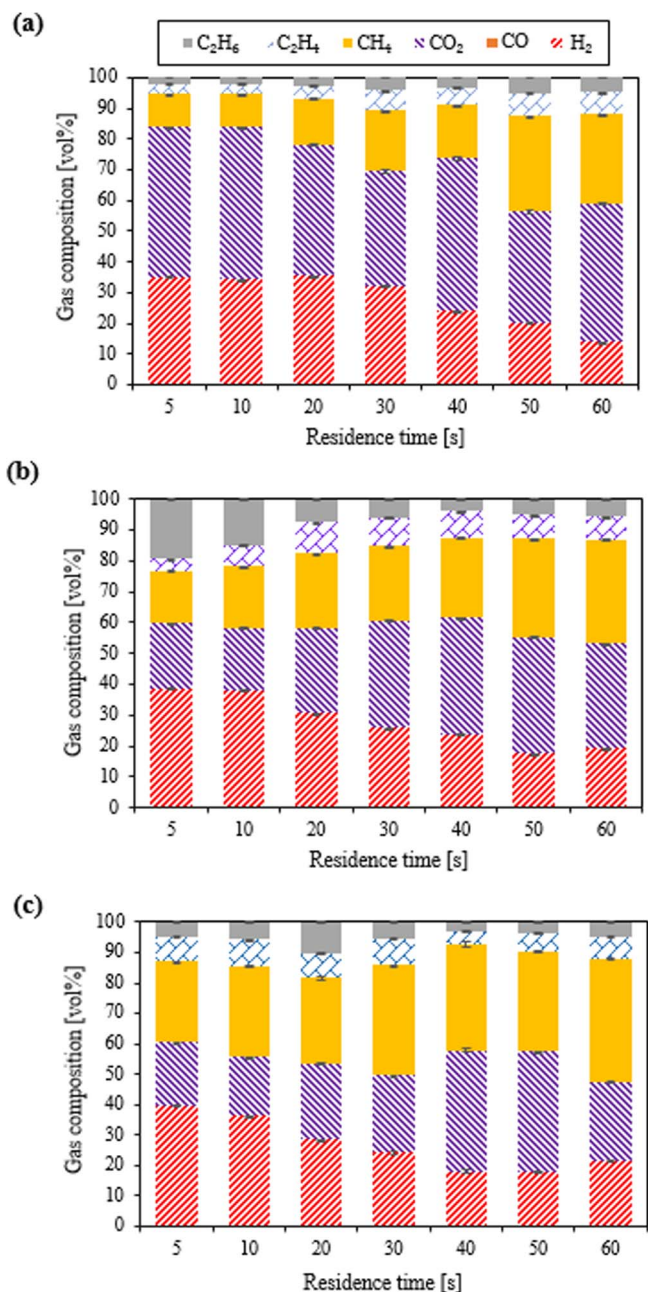
(a)

(b)

(c)

Fig. 4. Gas composition during SCWG of sewage sludge at the reaction temperature of (a) 500 °C, (b) 550 °C, and (c) 600 °C.

Table 1
Effect of temperature and time on CGE.

Residence time	CGE [−]		
[s]	500 °C	550 °C	600 °C
5	0.41 ± 0.000	0.63 ± 0.001	0.59 ± 0.001
10	0.41 ± 0.001	0.60 ± 0.003	0.60 ± 0.003
20	0.46 ± 0.000	0.62 ± 0.000	0.64 ± 0.010
30	0.50 ± 0.003	0.64 ± 0.003	0.72 ± 0.006
40	0.53 ± 0.004	0.66 ± 0.002	0.72 ± 0.001
50	0.57 ± 0.003	0.71 ± 0.002	0.74 ± 0.009
60	0.57 ± 0.000	0.70 ± 0.000	0.73 ± 0.005

analyzed to determine the phosphorus left in the reactor (remaining IP), and its yield was determined similarly.

The gaseous products were analyzed by using a gas chromatograph (GC) equipped with a thermal conductivity detector (TCD) and a flame ionization detector (FID). H_2 was detected by GC-TCD with N_2 as the carrier gas; CO_2 and CO were detected by GC-TCD with He as the carrier gas, and CH_4, C_2H_4, and C_2H_6 were detected by GC-FID with He as the carrier gas. The solid product particles trapped in the inline filter were removed, placed in a porcelain crucible, dried overnight in an oven, placed in a desiccator for 30 min, and then weighed until a constant weight was reached.

The carbon gasification efficiency (CGE) for each experimental run was calculated based on the carbon content in the feedstock, as indicated in Eq. (4):

$$CGE[-] = \frac{n_{gas} + n_{IC}}{n_{feedstock}} \quad (4)$$

where n_{gas} is the total amount of carbon present in the gaseous products [mol], n_{IC} is the total amount of inorganic carbon present in the liquid effluent [mol], and $n_{feedstock}$ is the total amount of carbon present in the initial feedstock [mol].

2.3. Reagents and Materials

All chemicals employed herein were used without further treatment or purification. Deionized water ($< 1 \mu S/cm$), used as solvent, was obtained by using a water deionizer (Organo, BB-5A). Sewage sludge, used as the feedstock for SCWG, was collected from a wastewater treatment plant in Higahashi-Hiroshima, Japan. The sewage sludge was filtered by using a suction filter and filter paper with a size of 11.0 cm (Whatman Grade 5 Qualitative). The sludge was then dried (80 °C, until constant weight), pulverized in a ball mill, and then sieved to a particle size of 40 μm. Water content and proximate analyses were performed by thermogravimetry (TG). Water content, VM, FC and ash was determined 79.16%, 77.5, 5.83 and 16.67 wt% respectively. Ultimate analysis of the sewage sludge was conducted previously (Unami et al., 2013). There were obtained CHNS-O, 43.1% C, 6.60% H, 4.42% N, 2.36% S and 25.9% O on dry weight basis.

3. Results and discussion

3.1. Yield of gas and liquid products

First, the carbon yields of the gas and liquid products is presented to confirm the reliability of the data. Fig. 2 shows the carbon yields of the gas and liquid products at 500, 550, and 600 °C. The obtained carbon balance for each experiment exceeded 0.8. When the temperature was increased from 500 to 600 °C, the carbon yield of the gaseous products increased rapidly, confirming that the generation of gaseous products was favored at high temperature. A longer residence time enhanced the formation of gaseous products. This is in good agreement with a previous study (Paksung and Matsumura, 2015) in which it was observed that the carbon yield of the gaseous products increased when the temperature exceeded a critical value (374 °C). As reported by another research group (Promdej and Matsumura, 2010; Guo et al., 2010), temperatures above the critical point of water result in a decrease in the density of water, thereby impeding the formation of ionic products. Because the formation of ionic products is impeded, the free radical mechanism is favored, resulting in higher gas yields. Notably, the formation of char was observed at 600 °C after 50 s. This might be due to the amount of lignin-like material in sewage sludge. Yong and Matsumura (2012) observed that char formation was enhanced under supercritical conditions in the case of lignin.

The phosphorus yield in the liquid products was also determined, as shown in Fig. 3. At the same temperature, the OP yield decreased with time, whereas the IP yield increased. The OP yield declined when the temperature was increased from 500 to 600 °C. The OP was mostly converted into IP in a short residence time of 5–10 s. Interestingly, the amount of remaining IP also increased with temperature and time. This
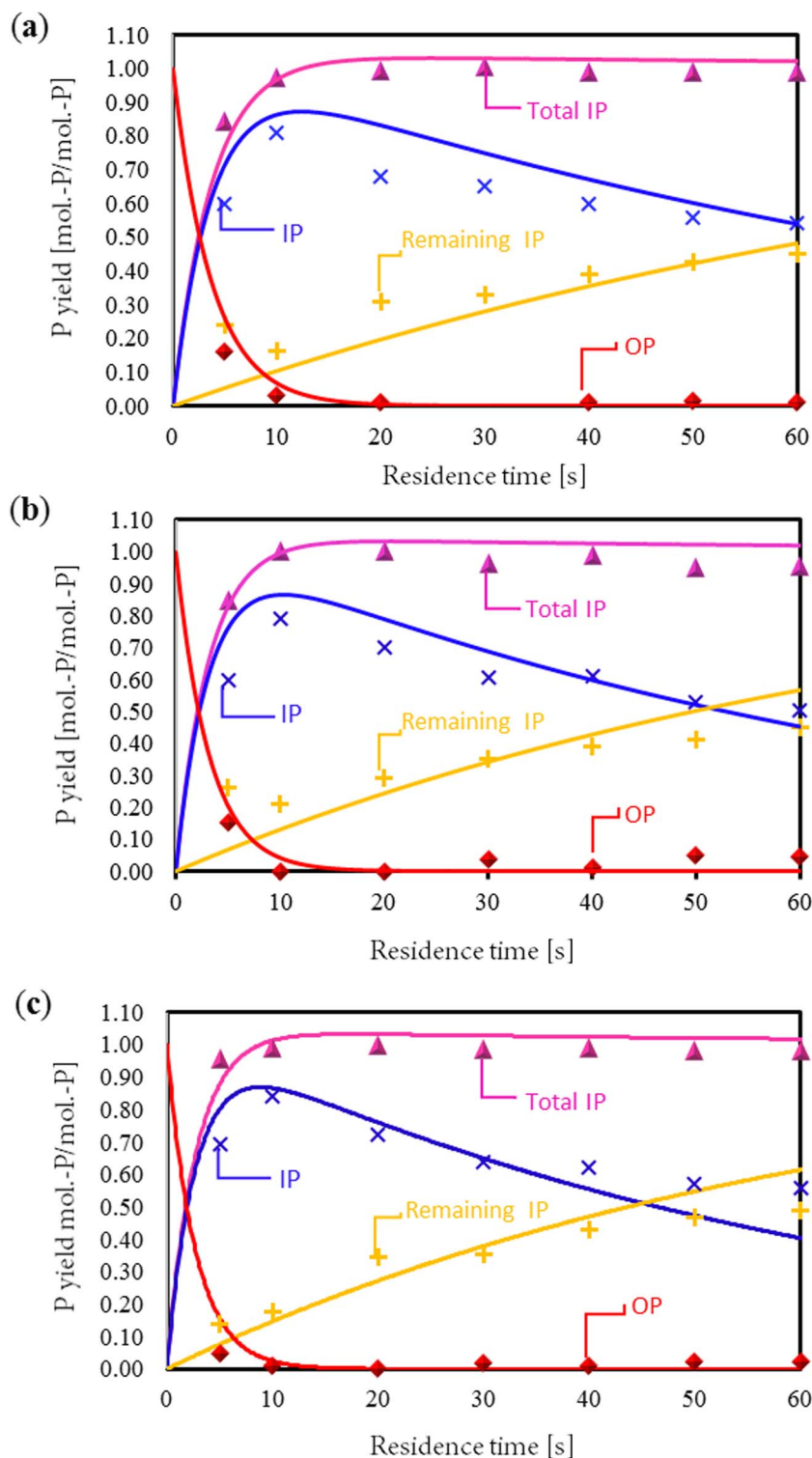
Fig. 5. Effect of temperature and residence time on behavior of phosphorus at (a) 500 °C, (b) 550 °C, (c) 600 °C. Symbol represent the experimental data and the lines the calculated data.

is in a good agreement with the previous work of Zhu et al. (2011) who observed a high percentage of remaining total phosphorus as a solid residue.

3.2. Effect of temperature and residence time on the product gas composition

Temperature can significantly affect the SCWG of sewage sludge. Fig. 4 shows the effect of temperature on the product gas composition during the SCWG of sewage sludge. The gaseous products were mainly composed of H_2, CO_2 and CH_4, and small quantities of C_2H_4 and C_2H_6. Intriguingly, no CO was found during the SCWG of sewage sludge under these experimental conditions (500–600 °C and 25 MPa). This finding is in agreement with a previous report (Gong et al., 2017) that no CO was detected during the SCWG of humic acid as a model compound of sewage sludge. A low yield of CO from SCWG was first pointed out by Xu et al. (1996).

At 500 °C, the main product was CO_2 (49.5 vol%) due to the decarboxylation reaction. This is in good agreement with previous research (Acelas et al., 2014), where it was reported that decarboxylation
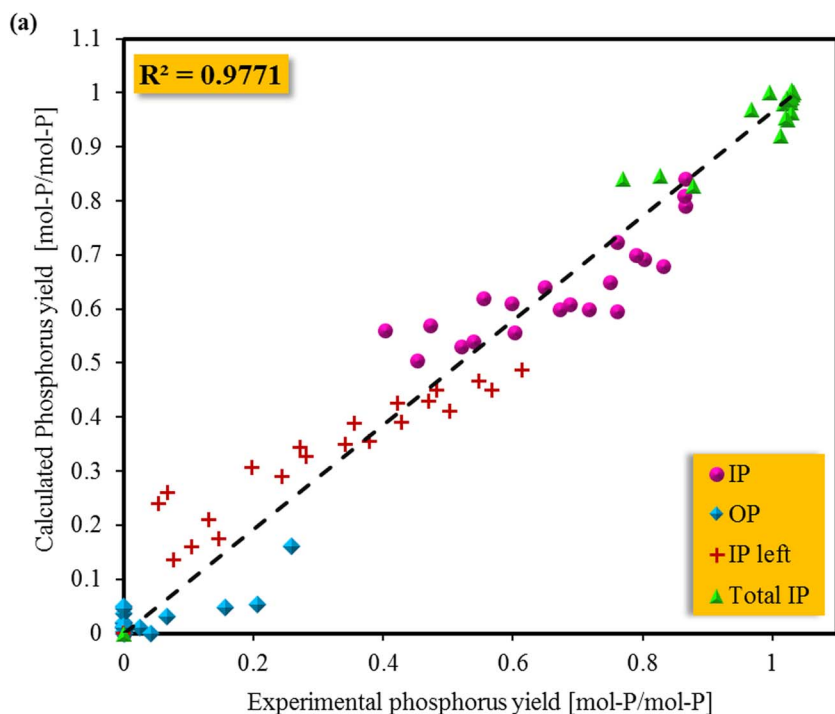
(a)

(b)

Fig. 6. (a) Comparison of experimental and calculated P yield in SCWG of sewage sludge (experimental conditions: 500–600 °C, 25 MPa, and 0.1 wt% of solid sewage sludge), (b) Arrhenius plot for P yield in SCWG of sewage sludge (experimental conditions: 500–600 °C, 25 MPa, and 0.1 wt% of solid sewage sludge).
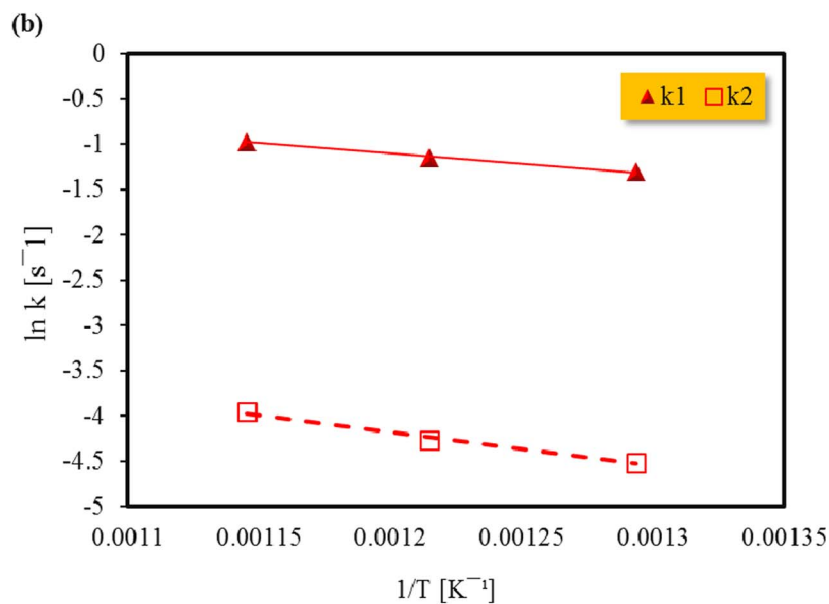
Table 2

Activation energies and pre-exponential factors (Experimental conditions: 500–600 °C, 25 MPa, and 0.1 wt% of solid sewage sludge).

Reaction direction	Reaction rate constant [s^{-1}]	Activation energy, E_a [kJ mol^{-1}]	Pre-exponential factor, A [s^{-1}]	R^2
OP → IP	k_1	19.1	5.21	0.993
IP → remaining IP	k_2	18.7	4.79	0.998

occurred at low temperature. When the reaction time increased, the CH$_4$ yield increased from 10.5 to 28.8 vol%. This is because methanation (Eq. (5)) is favored at long residence time. Concomitantly, the H$_2$ yield decreased from 35.1 to 13.9 vol% with time due to the reaction of CO with H$_2$ to generate CH$_4$.

$$CO + 3H_2 \leftrightarrow CH_4 + H_2O \tag{5}$$

At higher temperatures (550 and 600 °C), H$_2$ was generated as the main product at short residence time is about 38.5–39.4 vol%. This is because the water-gas shift reaction (Eq. (6)) is favored at high temperature. Another possible route for H$_2$ formation is the thermal decomposition of the intermediate compounds (Acelas et al., 2014). At all temperatures (500–600 °C), the CH$_4$ yield increased with time, confirming that methanation was favored when the residence time was prolonged. This is in line with a previous report (Byrd et al., 2008) that the CH$_4$ yield increased with time. Overall, the trends in the product gas composition of sewage sludge observed in this study are in good

agreement with those reported in the literature (Acelas et al., 2014; Matsumura et al., 2013; Wilkinson et al., 2012).

$$CO + H_2O \Leftrightarrow CO_2 + H_2 \qquad (6)$$

Table 1 shows the effect of the reaction temperature and time on the carbon gasification efficiency (CGE) for sewage sludge. The CGE increased with temperature and time. As reported by Shoji et al. (2006), Lu et al. (2006), and Guo et al. (2007), the reaction rate of gasification was accelerated with increasing temperature. The increase in the CGE with time and temperature is also in good agreement with the documented trends (Samanmulya et al., 2017; Yong and Matsumura, 2012).

3.3. Detailed reaction kinetics of sewage sludge SCWG

In previous studies, the kinetics of sewage sludge pyrolysis were thoroughly investigated (Lundberg et al., 2015; Nowicki et al., 2011; Shao et al., 2008). Lundberg et al., developed three kinetics models which are the grain model, the random pore model, and an empirical model. The empirical model is the only one which gave satisfactory agreement with the experimental data. Nowicki et al. (2011) determined the first-order kinetics parameters from experimental data for steam gasification of the char. Shao et al. (2008) studied pyrolysis characteristics and kinetics of sewage sludge by thermogravimetry Fourier Transform Infrared Analysis and they found the calculated kinetic parameters explained the observed pyrolysis characteristics well. However, the detailed kinetics for the conversion of OP to IP in the liquid products generated via the SCWG have not been well studied. Determination of these reaction kinetics is important for elucidating the detailed mechanistic of phosphorus conversion during the SCWG of sewage sludge. Based on the phosphorus yield presented in Section 3.1, it is confirmed that there are two consecutive reaction steps. First, the OP was converted to IP. This is a rather quick reaction that takes only 10 s. Secondly, IP was converted into solid phase inorganic phosphorus that remained in the reactor (remaining IP). The models can be expressed by the following equation.

$$OP \xrightarrow{k_1} IP \xrightarrow{k_2} (remaining\ IP) \qquad (7)$$

The rate of change of the yield of each compound can be expressed by the differential rate equations shown in Eqs. (8)–(10).

$$\frac{d[OP]}{dt} = -k_1[OP] \qquad (8)$$

$$\frac{d[IP]}{dt} = k_1[OP] - k_2[IP] \qquad (9)$$

$$\frac{d[remaining\ IP]}{dt} = k_2[IP] \qquad (10)$$

Integrating Eq. (8) gives:

$$[OP] = [OP]_0 \exp(-k_1 t) \qquad (11)$$

Substituting Eq. (11) into Eq. (9) gives:

$$[IP] = \frac{k_1}{k_2 - k_1}[OP]_0\{\exp(-k_1 t) - \exp(-k_2 t)\} \qquad (12)$$

Finally,

$$[remaining\ IP] = [OP]_0 - [OP] - [IP], \qquad (13)$$

thus [remaining IP] was determined using:

$$[remaining\ IP] = [OP]_0\left[1 + \frac{k_1\exp(-k_2 t) - k_2\exp(-k_1 t)}{k_2 - k_1}\right] \qquad (14)$$

Because the OP was rapidly converted to IP, which was then slowly consumed to generate remaining IP, Eq. (14) can be approximated as:

$$[remaining\ IP] = [OP]_0[1 - \exp(-k_2 t)] \qquad (15)$$

where k_i is the reaction rate constant $[s^{-1}]$, t is the residence time [s],

and [X] is the concentration of component X [mol]. The calculated concentration of OP, IP, and remaining IP are depicted in Fig. 5, along with the experimental values. The reaction rate constants were determined by using non-linear regression with the least squares error (LSE) method (i.e., the squared difference between the experimental and calculated values was minimized so that the corresponding constants gave the best fit between the experimental data and calculated values). Fig. 6(a) shows the parity plot comparing the experimental data for the compound concentration with the values calculated with the model employing the LSE method. On the basis of the graph and as suggested by the high coefficient of determination (R^2), the model predictions appear to fit the experimental data fairly well.

The temperature-dependence of the reaction rate constants was then modeled by using the Arrhenius equation, in order to determine the activation energy and pre-exponential factor. Fig. 6(b) displays the Arrhenius plots of the individual rate constants for phosphorus production during the SCWG of sewage sludge. This figure shows the straight line fit of ln k versus $1/T$, from which the activation energy E_a and pre-exponential factor A could be determined.

Table 2 shows the E_a and A for the detailed kinetic analysis of the SCWG of sewage sludge. The activation energies for the conversion of OP to IP and IP to remaining IP were determined as 19.1 and 18.7 kJ mol^{-1}, respectively. The pre-exponential factors for the conversion of OP to IP and IP to remaining IP were about 5.21 and 4.79 s^{-1}, respectively.

4. Conclusion

A process for the simultaneous conversion of sewage sludge into gaseous products and the recovery of phosphorus from SCWG was investigated. The gaseous products were mainly composed of H$_2$, CO$_2$, and CH$_4$. A CGE as high as 0.73 was achieved at 600 °C after 50 s. OP was rapidly converted into IP at short residence time (10 s). The developed kinetic model was found to fit well to the experimental data. The activation energies for the conversion of OP to IP and IP to remaining IP in the SCWG of sewage sludge were approximately 19.1 and 18.7 kJ mol^{-1}, respectively. The pre-exponential factors for the conversion of OP to IP and IP to remaining IP were about 5.21 and 4.79 s^{-1}, respectively.

Acknowledgements

References

Acelas, N.Y., Lpez, D.P., Wim Brilman, D.W.F., Kersten, S.R.A., Kootstra, A.M.J., 2014. Supercritical water gasification of sewage sludge: Gas production and phosphorus recovery. Bioresour. Technol. 174, 167–175. http://dx.doi.org/10.1016/j.biortech.2014.10.003.

Arakane, M., Imai, T., Murakami, S., Takeuchi, M., Ukita, M., Sekine, M., Higuchi, T., 2005. Resource recovery from excess sludge by subcritical water process with magnesium ammonium phosphate process. J. Water Environ. Technol. 3, 119–124. http://dx.doi.org/10.2965/jwet.2005.119.

Blöcher, C., Niewersch, C., Melin, T., 2012. Phosphorus recovery from sewage sludge with a hybrid process of low pressure wet oxidation and nanofiltration. Water Res. 46, 2009–2019. http://dx.doi.org/10.1016/j.watres.2012.01.022.

Byrd, A.J., Pant, K.K., Gupta, R.B., 2008. Hydrogen production from glycerol by reforming in supercritical water over Ru/Al2O3 catalyst. Fuel 87, 2956–2960. http://dx.doi.org/10.1016/j.fuel.2008.04.024.

Deng, S., Tan, H., Wang, X., Yang, F., Cao, R., Wang, Z., Ruan, R., 2017. Investigation on the fast co-pyrolysis of sewage sludge with biomass and the combustion reactivity of residual char. Bioresour. Technol. 239, 302–310. http://dx.doi.org/10.1016/j.biortech.2017.04.067.

Farobie, O., Changkiendee, P., Inoue, S., Inoue, T., Kawai, Y., Noguchi, T., Tanigawa, H., Matsumura, Y., 2017. Effect of the heating rate on the supercritical water gasification of a glucose/guaiacol mixture. Ind. Eng. Chem. Res. 56, 6401–6407. http://dx.doi.org/10.1021/acs.iecr.7b00640.

Gong, M., Nanda, S., Romero, M.J., Zhu, W., Kozinski, J.A., 2017. Subcritical and supercritical water gasification of humic acid as a model compound of humic substances in sewage sludge. J. Supercrit. Fluids 119, 130–138. http://dx.doi.org/10.1016/j.supflu.2016.08.018.

Gong, M., Zhu, W., Fan, Y., Zhang, H., Su, Y., 2016. Influence of the reactant carbon-hydrogen-oxygen composition on the key products of the direct gasification of dewatered sewage sludge in supercritical water. Bioresour. Technol. http://dx.doi.org/10.1016/j.biortech.2016.02.070.

Goto, M., Nada, T., Kodama, A., Hirose, T., 1999. Kinetic Analysis for destruction of municipal sewage sludge and alcohol distillery wastewater by supercritical water oxidation. Ind. Eng. Chem. Res. 38, 1863–1865. http://dx.doi.org/10.1021/ie980479s.

Guo, L.J., Lu, Y.J., Zhang, X.M., Ji, C.M., Guan, Y., Pei, A.X., 2007. Hydrogen production by biomass gasification in supercritical water: a systematic experimental and analytical study. Catal. Today 129, 275–286. http://dx.doi.org/10.1016/j.cattod.2007.05.027.

Guo, Y., Wang, S.Z., Xu, D.H., Gong, Y.M., Ma, H.H., Tang, X.Y., 2010. Review of catalytic supercritical water gasification for hydrogen production from biomass. Renewable Sustainable Energy Rev. 14, 334–343. http://dx.doi.org/10.1016/j.rser.2009.08.012.

Han, H., Hu, S., Syed-Hassan, S.S.A., Xiao, Y., Wang, Y., Xu, J., Jiang, L., Su, S., Xiang, J., 2017. Effects of reaction conditions on the emission behaviors of arsenic, cadmium and lead during sewage sludge pyrolysis. Bioresour. Technol. 236, 138–145. http://dx.doi.org/10.1016/j.biortech.2017.03.112.

He, C., Chen, C.L., Giannis, A., Yang, Y., Wang, J.Y., 2014. Hydrothermal gasification of sewage sludge and model compounds for renewable hydrogen production: a review. Renewable Sustainable Energy Rev. 39, 1127–1142. http://dx.doi.org/10.1016/j.rser.2014.07.141.

Kruse, A., Dinjus, E., 2007. Hot compressed water as reaction medium and reactant. 2 Degradation reactions. J. Supercrit. Fluids 41, 361–379. http://dx.doi.org/10.1016/j.supflu.2006.12.006.

Liu, T., Guo, Y., Peng, N., Lang, Q., Xia, Y., Gai, C., Liu, Z., 2017. Nitrogen transformation among char, tar and gas during pyrolysis of sewage sludge and corresponding hydrochar. J. Anal. Appl. Pyrolysis 0–1. http://dx.doi.org/10.1016/j.jaap.2017.05.017.

Lu, Y.J., Guo, L.J., Ji, C.M., Zhang, X.M., Hao, X.H., Yan, Q.H., 2006. Hydrogen production by biomass gasification in supercritical water: a parametric study. Int. J. Hydrogen Energy 31, 822–831. http://dx.doi.org/10.1016/j.ijhydene.2005.08.011.

Lundberg, L., Tchoffor, P.A., Johansson, R., Pallarès, D., 2015. Determination of kinetic parameters for the gasification of biomass char using a bubbling fluidised bed reactor, In: Proceedings of the 22nd International Conference on Fluidized Bed Conversion, Jun. 14-17, 2015, Turku, Finland, pp.456–464.

Matsumura, Y., Minowa, T., Potic, B., Kersten, S.R.A., Prins, W., Van Swaaij, W.P.M., Van De Beld, B., Elliott, D.C., Neuenschwander, G.G., Kruse, A., Antal, M.J., 2005. Biomass gasification in near- and super-critical water: status and prospects. Biomass Bioenergy 29, 269–292. http://dx.doi.org/10.1016/j.biombioe.2005.04.006.

Matsumura, Y., Hara, S., Kaminaka, K., Yamashita, Y., Yoshida, T., 2013. Gasification rate of various biomass feedstocks in supercritical water. J. Jpn. Petrol. Inst. 56, 1–10 doi.org/10.1627/jpi.56.1.

Nowicki, L., Antecka, A., Bedyk, T., Stolarek, P., Ledakowicz, S., 2011. The kinetics of gasification of char derived from sewage sludge. J. Therm. Anal. Calorim. 104, 693–700. http://dx.doi.org/10.1007/s10973-010-1032-1.

Paksung, N., Matsumura, Y., 2015. Decomposition of xylose in sub- and supercritical water. Ind. Eng. Chem. Res. 54, 7604–7613. http://dx.doi.org/10.1021/acs.iecr.5b01623.

Petzet, S., Peplinski, B., Cornel, P., 2012. On wet chemical phosphorus recovery from sewage sludge ash by acidic or alkaline leaching and an optimized combination of both. Water Res. 46, 3769–3780. http://dx.doi.org/10.1016/j.watres.2012.03.068.

Promdej, C., Matsumura, Y., 2010. Effect of temperature on tarry material production of glucose in supercritical water gasification. J. Jpn. Inst. Energy 89, 1179–1184. http://dx.doi.org/10.3775/jie.89.1179.

Qian, L., Wang, S., Savage, P.E., 2017. Hydrothermal liquefaction of sewage sludge under isothermal and fast conditions. Bioresour. Technol. 232, 27–34. http://dx.doi.org/10.1016/j.biortech.2017.02.017.

Samanmulya, T., Farobie, O., Matsumura, Y., 2017. Gasification characteristics of aminobutyric acid and serine as model compounds of proteins under supercritical water conditions. J. Japan Pet. Inst. 60, 34–40. http://dx.doi.org/10.1627/jpi.60.34.

Shao, J., Yan, R., Chen, H., Wang, B., Ho Lee, D., Tee Liang, D., 2008. Pyrolysis characteristics and kinetics of sewage sludge by thermogravimetry fourier transform infrared analysis. Energy Fuels 22, 38–45. http://dx.doi.org/10.1021/ef700287p.

Shoji, D., Kuramochi, N., Yui, K., Uchida, H., Itatani, K., Koda, S., 2006. Visualized kinetic aspects of a wood block in sub- and supercritical water oxidation. Ind. Eng. Chem. Res. 45, 5885–5890. http://dx.doi.org/10.1021/ie0604775.

Unami, Y., Kanna, M., Yanagida, T., Matsumura, Y., 2013. Phosphorus recovery by supercritical water gasification of sewage sludge, Pa-216, In: Proc. 8th Conference on Biomass Science, Higashi-Hiroshima, Jan. 9-10, 2013, Higashi-Hiroshima, Japan (in Japanese). doi: 10.20550/jiebiomassronbun.8.0_110.

Wilkinson, N., Wickramathilaka, M., Hendry, D., Miller, A., Espanani, R., Jacoby, W., 2012. Rate determination of supercritical water gasification of primary sewage sludge as a replacement for anaerobic digestion. Bioresour. Technol. 124, 269–275. http://dx.doi.org/10.1016/j.biortech.2012.08.011.

Xu, X., Matsumura, Y., Stenberg, J., Antal Jr., M.J., 1996. Carbon catalysed gasification of organic feedstocks in supercritical water. Ind. Eng. Chem. Res. 35, 2522–2530. http://dx.doi.org/10.1021/ie950672b.

Xu, Z.R., Zhu, W., Gong, M., Zhang, H.W., 2013. Direct gasification of dewatered sewage sludge in supercritical water. Part 1: effects of alkali salts. Int. J. Hydrogen Energy 38, 3963–3972. http://dx.doi.org/10.1016/j.ijhydene.2013.01.164.

Yanagida, T., Minowa, T., Nakamura, A., Matsumura, Y., Noda, Y., 2008. Behavior of inorganic elements in poultry manure during supercritical water gasification. Nihon Enerugi Gakkaishi/J. Jpn Inst. Energy 10.3775/jie.87.731.

Yong, T.L.K., Matsumura, Y., 2012. Catalytic gasification of poultry manure and eucalyptus wood mixture in supercritical water. Ind. Eng. Chem. Res. 51, 5685–5690. http://dx.doi.org/10.1021/ie202385s.

Yuan, Z., Pratt, S., Batstone, D.J., 2012. Phosphorus recovery from wastewater through microbial processes. Curr. Opin. Biotechnol. 23, 878–883. http://dx.doi.org/10.1016/j.copbio.2012.08.001.

Zhang, L., Xu, C.Charles., Champagne, P., 2010. Energy recovery from secondary pulp/paper-mill sludge and sewage sludge with supercritical water treatment. Bioresour. Technol. 101, 2713–2721. http://dx.doi.org/10.1016/j.biortech.2009.11.106.

Zhu, W., Xu, Z.R., Li, L., He, C., 2011. The behavior of phosphorus in sub- and supercritical water gasification of sewage sludge. Chem. Eng. J 10.1016/j.cej.2011.03.090.